AD-A132 365 DETERMINING STRESSES IN THE PRESENCE OF NONLINEARITIES IN INTERPLANAR SPA..(U) NORTHWESTERN UNIV EVANSTON IL DEPT OF MATERIALS SCIENCE I C NOYAN ET AL. 29 JUL 83 1/1

UNCLASSIFIED TR-10 N00014-80-C-0116 F/G 20/12 NL

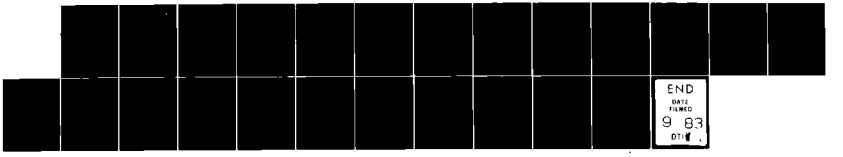

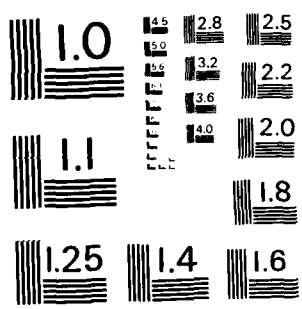

13

NORTHWESTERN UNIVERSITY

DEPARTMENT OF MATERIALS SCIENCE

Technical Report No. 10
July 29, 1983

Office of Naval Research
Contract N00014-80-C-0116

DETERMINING STRESSES IN THE PRESENCE OF NONLINEARITIES IN INTERPLANAR SPACING VS. SIN$^2\psi$

BY

I. C. Noyan and J. B. Cohen

EVANSTON, ILLINOIS

DETERMINING STRESSES IN THE PRESENCE OF NONLINEARITIES IN INTER-PLANAR SPACING VS. $SIN^2\psi$.

I. C. Noyan and J. B. Cohen

I. C. Noyan is research assistant and graduate student, J. B. Cohen is Frank C.Engelhart Professor of Materials Science and Engineering and Technological Institute Professor

Northwestern University, Dept. of Mat. Sci. and Eng., Technological Institute, Evanston, Il. 60201

ABSTRACT

The physical meaning of non-linearities in "d" vs. $\sin^2\psi$ lines, encountered in X-ray measurements of surface residual stresses in polycrystalline materials is investigated. It is shown that when oscillations are present in any one reflection, switching to another reflection to obtain a straight line in "d" vs. $\sin^2\psi$ is feasible only under very special conditions. We also discuss the effect of "quasi-homogeneous" strain distributions and investigate the effects of ψ-range on the accuracy of X-ray residual stress measurements when "ψ-splitting" is present. A new geometric error is also discussed that can not be detected by the "annealed powder" method often used for alignment.

Introduction

In the past few years the basic equations used for the determination of surface residual stresses in polycrystalline materials by X-rays have undergone considerable modification and expansion. Traditional methods assume a bi-axial stress state that is uniform in the surface layers penetrated by the X-ray beam[1,2]. This assumption is based on the concept that this penetration depth is too shallow to be affected by the stresses in the third dimension. Methods based on this assumption predict a linear variation of interplanar spacing "d" with $\sin^2\psi$, with a slope that is proportional to the stress in the measurement direction S_ϕ; here ϕ is the angle between the normal of the diffracting planes $\underline{L_3}$ and the surface normal of the specimen $\underline{S_3}$, as shown in figure 1. If the components of the (assumed) bi-axial stress tensor exhibit steep gradients in the volume sampled by the X-ray beam, curvature occurs in the "d" vs. $\sin^2\psi$ plot. The slope of a least squares fit to such data yields the stress in the $\underline{S_\phi}$ direction, averaged over the depth of penetration[3].

The assumption in these traditional methods, that stress components in the direction of the surface normal are negligible in the volume sampled by the X-ray beam was shown to be invalid in several recent studies[4,5,6]. Stress components of appreciable magnitude in this direction have been detected in the surface layers of materials prepared in certain ways. Recent theory as well as experiment show that, when only the normal stress σ_{33} is present in the direction of the surface normal, curvature occurs in the "d" vs. $\sin^2\psi$ data[7,8]. The degree of such curvature depends on the steepness of the gradient in σ_{33}. It has also been shown that even for very small curvature in "d" vs. $\sin^2\psi$ data, analysis with the bi-axial assumption causes appreciable error in the calculated surface stress, and that a high ψ-range ($\sin^2\psi \geq .4$) should be used even when tri-axial analyses, (taking into account the presence of σ_{33}) are employed. When the shear stresses σ_{13} σ_{23} are present in the measurement volume, splitting of the "d" vs. $\sin^2\psi$ data results; that is, "d" vs. $\sin^2\psi$ plots have opposite curvature for negative and positive ψ. Analysis of such data has been described in detail by Dolle. (see also references 4,5 for the use of this analysis). We present here the first study of the effect of ψ-range on the accuracy of this analysis.

Both the traditional methods and the methods that have been expanded to include the effect of the stresses in the direction of the surface normal predict a smooth variation in the "d" vs. $\sin^2\psi$ curves with no large oscillations. However such oscillations are often encountered in practice and various explanations have been given for their cause[6,10,11]. The latest study attributes the cause of oscillations to elastic anisotropy (i.e change in the elastic constants of the material with each ψ-tilt), and suggests the use of h00 and hhh type reflections for

X-ray residual stress analysis when oscillations are present in the hkl type reflections, since calculations indicate that the elastic constants associated with such reflections are isotropic .

In this paper we will investigate the effects of the ψ-range on the accuracy of residual stress results determined by X-rays when ψ-splitting is present. It will be shown that the ψ-range is very important and must be chosen according to the stress gradient(s) existing in σ_{13} and/or σ_{23}. Information about the gradient can be obtained from a plot of "a_2" vs. $\sin|2\psi|$ (where $a_2=\frac{1}{2}(d_{\phi\psi^+}-d_{\phi\psi^-})$). Furthermore a geometric error will be discussed which causes ψ-splitting of the same shape as that caused by the presence of σ_{13} and/or σ_{23}. This error can not be detected by the current "annealed- powder" alignment technique used to minimize geometric contributions to the observed "ψ-splitting". We will also examine the presence of oscillations in "d" vs. $\sin^2\psi$ and show that oscillations are expected in h00 and hhh reflections when they are present in the hkl reflections. Computer simulation and experimental data are presented to test the above ideas.

The Basic Equations

The orthogonal coordinate systems used in the following discussion are shown in figure 1. The specimen axes are defined such that $\underline{S}_1$, $\underline{S}_2$ are in the plane of the specimen surface. The laboratory system, in which diffraction is occurring, is defined such that $\underline{L}_3$ is in the direction of the normal to the family of planes (hkl) whose "d" spacings are being measured by X-rays. $\underline{L}_3$ is in the plane defined by $\underline{S}_1$ and $\underline{S}_2$ and makes an angle ϕ with $\underline{S}_2$. In what follows, primed tensor quantities refer to the laboratory system $\underline{L}_i$ and unprimed quantities to the sample system $\underline{S}_i$, following the convention established by Dölle[6].

If the unstressed lattice spacing "do" for the material under examination is known, strains in the $\underline{L}_3$ direction may be obtained from the formula :

$$(\epsilon'_{33}) = (d_{\phi\psi}-do)/do \ . \qquad (1)$$

this strain may be expressed in terms of the strains in the $\underline{S}_i$ coordinate system using the tensor transformation :

$$(\epsilon'_{33})_{\phi\psi} = a_{3k}a_{3l}\epsilon_{kl} \qquad (2\text{-a})$$

where a_{3k} , a_{3l} are the direction cosines between the axes $\underline{L}_3$ and $\underline{S}_k$ or $\underline{S}_l$ respectively. For arbitrary angles ϕ and ψ (2-a)

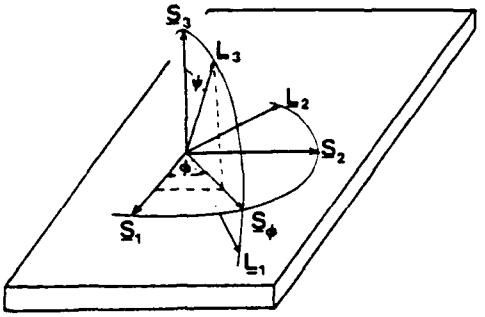

FIGURE 1: Definition of the angles and orientation of the laboratory system $\underline{L}_i$ with respect to the sample system $\underline{S}_i$.

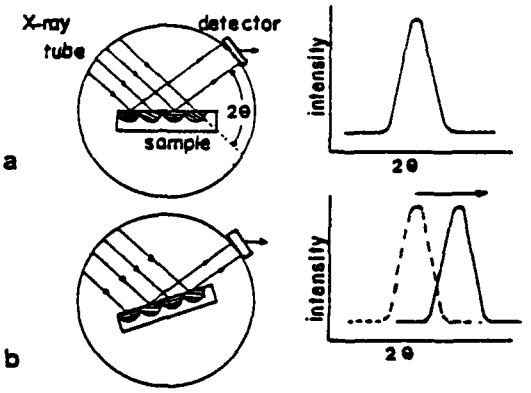

Figure 2: Schematic of a diffractometer in a stress measurement. a) Certain atomic planes satisfy Bragg's law and diffract X-rays at a value which depends on the spacing of the planes. This spacing is affected by the stresses existing in the surface layers. b) After the specimen is tilted, diffraction occurs from other grains but from the same set of planes. Since the normal stress component on these is different than in (a), the plane spacing will be different, as will the diffraction angle.

becomes :

$$(\epsilon'_{33})_{\phi\psi} = [\epsilon_{11}\cos^2\phi + \epsilon_{12}\sin 2\phi + \epsilon_{22}\sin^2\phi - \epsilon_{33}]\sin^2\psi - \epsilon_{33}$$

$$+ (\epsilon_{13}\cos\phi + \epsilon_{23}\sin\phi)\sin 2\psi \qquad (2\text{-b})$$

Once the strains in $\underline{S}_i$ are obtained (by techniques described in reference 6, or by least squares solution), one can obtain the stresses in the sample coordinate system from:

$$\sigma_{ij} = C_{ijkl}\epsilon_{kl} \qquad (3)$$

Where C_{ijkl} are the stiffness coefficients of the material, referred to the $\underline{S}_i$ coordinate system.

Presence of Oscillations

It must be noted that the above development makes no assumptions about whether the material under investigation is polycrystalline or is a single crystal. It is valid for both isotropic and anisotropic materials, and predicts a linear "d" vs. $\sin^2\psi$ behaviour (for ϵ_{13}, $\epsilon_{23} = 0$) or regular "ψ-splitting" (ϵ_{13} and/or $\epsilon_{23} \neq 0$). There are however two implicit assumptions in the above treatment[12]:

(i) The strain tensor for the material under examination is a symmetrical second rank tensor.

(ii) The strains ϵ_{kl} in the specimen coordinate system $\underline{S}_i$ are homogeneous in the total diffraction volume sampled during the experiment.

The second assumption is very important for X-ray residual stress determination in polycrystalline specimens. It is well known that the grains that contribute to the diffraction profile (from which "$d_{\phi\psi}$" is determined) are different for every ψ-tilt (figure 2*). Thus, when we use the $(\epsilon'_{33})_{\phi\psi}$, determined from these mutually exclusive subsets of the total irradiated volume to calculate the strain tensor for the surface coordinate system $\underline{S}_i$, we are assuming, a-priori, that ϵ_{kl} in the coordinate system $\underline{S}_i$ is invariant (i.e. homogeneous) no matter where the origin of $\underline{S}_i$ is located within the total irradiated volume. An experimentally determined linear "$d_{\phi\psi}$" vs. $\sin^2\psi$ plot means that this assumption is justified and equation 2 is valid for the volume of material examined. On the other hand, oscillations in "$d_{\phi\psi}$" vs. $\sin^2\psi$ mean that an inhomogeneous strain distribution exists at the surface, with each diffracting subset having their unique strain tensor (ϵ_{kl}) for the coordinate system $\underline{S}_i$. In such a case the strain along a given direction in the sample coordinate system will be different at different points and this will cause non-uniform strain gradients in the irradiated volume whose variation increases with increasing oscillations in "$d_{\phi\psi}$" vs.

$\sin^2\psi$. It is rather improbable to have certain grains in the irradiated volume that are free from the effect of these gradients, which is the assumption made when switching to an h00 and hhh reflection (without moving the beam position) after observing oscillations in an hkl reflection. Consider figure 3; When oscillations are present in "$d\phi\psi$" vs. $\sin^2\psi$ for the hkl reflection, ϵ_{kl} are different at points 1,3,5. In order for "$d\phi\psi$" vs. $\sin^2\psi$ to be linear for the hhh reflection, ϵ_{kl} should be constant at points 2,4,6. When grain size is small and the gradients are steep (i.e, large oscillations), this is probable if the inhomogeneous regions have a very small mean size and volume fraction. Otherwise all points will have large, non-uniform gradients in order to keep the displacements constant across grain boundaries in the measurement volume. Thus one would expect oscillations in all reflections when large oscillations are present in any one reflection.

In figure 4 the "$d\phi\psi$" vs. $\sin^2\psi$ plots from a cold-rolled (90%) α-brass specimen, which was then polished to .05 microns (diamond paste), are shown for various elastic loads applied in-situ on a diffractometer. Also shown, as a measure of texture are the relative intensities of the X-ray peak for each ψ-tilt. It is seen that the material has texture, and oscillations occur for both (222) and (311) reflections. This result can not be explained by the "elastic anisotropy" concepts developed in references [6,7]. In a previous paper Dölle and Cohen[3] concluded otherwise but the h00 reflection used was at low 2θ angle ($\sim 105^\circ 2\theta$) where any oscillations would be harder to detect (since $\Delta d/d = -\cot\theta \cdot \Delta 2\theta/2$).

The origin of the non-uniform strain gradients, (and hence the reason for the oscillations) is not important for the arguements presented above. Such gradients may arise from inhomogeneous stress gradients[11], inhomogeneous plastic flow in the volume under examination[10,18,16,17], or changes in the elastic constants s, s of the material in various subsets of the total irradiated volume. This last effect may be due to large grains oriented differently, texture[3], or the presence of other phases with different elastic constants[9]. When an elastic stress is applied at the boundaries of such materials it will cause a reaction stress field which acts to keep the displacements constant across phase (or grain) boundaries . Such a reaction stress field will be inhomogeneous[19], and thus, cause oscillations . For a given applied stress the inhomogeneity will be more pronounced (and the oscillations larger) in the phases that have a smaller volume fraction and small grain sizes.

Different methods have been proposed so far to obtain the stress state in the surface layers for some of the cases listed above. However so far no combined method that is rigorously

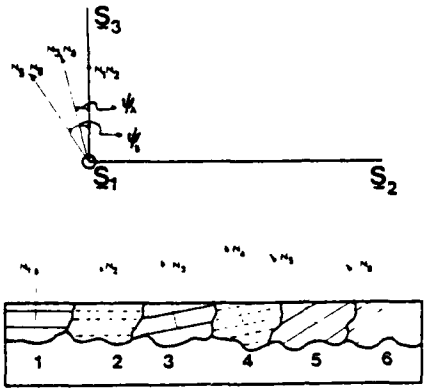

Figure 3: Hypothetical specimen whose grains 1, 3, 5 and 2, 4, 6 will diffract at $\psi = 0$, ψ_A, ψ_B, for hkl and hhh reflections respectively.

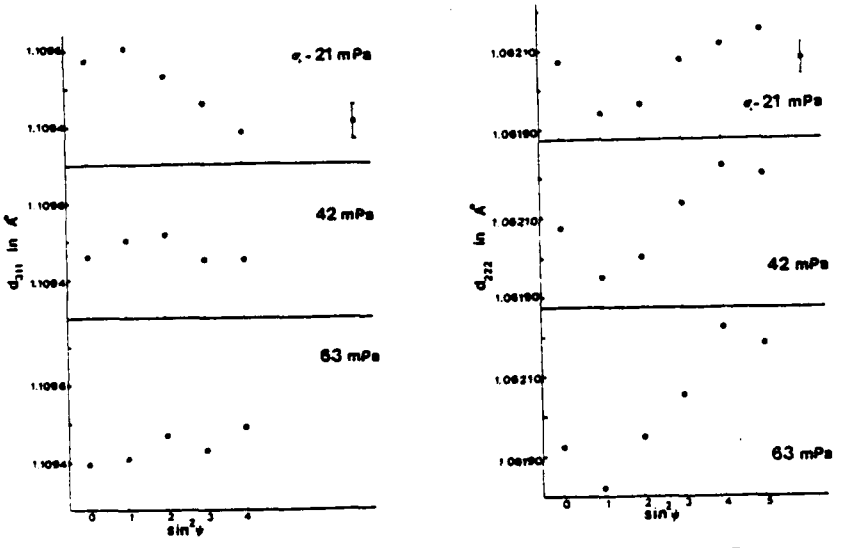

Figure 4: Interplanar spacing "d" vs. $\sin^2\psi$ lines obtained from a cold-rolled alpha-brass specimen (using filtered Fe-K radiation and a solid-state detector to reduce the background due to fluorescence). The specimen was loaded to a different elastic load for each measurement.
a) "d" vs. $\sin^2\psi$ data for 311 reflection (128° 2θ) at loads 21, 42, 63 mPa.
b) "d" vs. $\sin^2\psi$ data for 222 reflection (131° 2θ) at the same loads.

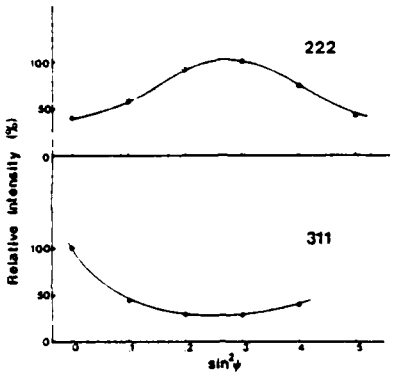

4c) Relative intensities for both reflections at each ψ-tilt show the presence of texture.

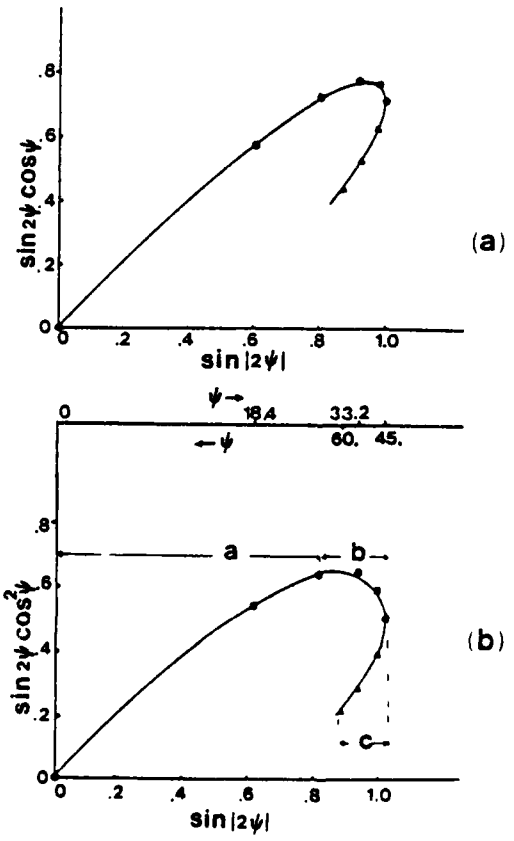

Figure 5: Variation of the function $\sin 2\psi(\cos\psi)^{n_{13}}$ over $\psi=(0,60)$ for $n_{13}=1$ (a) and $n_{13}=2$ (b).

based on elasticity theory is available. Such a method is under investigation at Northwestern University and will be reported at a later date.

ψ-Splitting In Isotropic Materials with Homogeneous Strain Fields

For isotropic materials equation (3) becomes[12]:

$$\sigma_{ij} = (1+\nu/E)\sigma_{ij} - \nu/E\delta_{ij}\epsilon_{kk} \qquad (4\text{-a})$$

or, inverting the equation and expressing strains in terms of stresses:

$$\epsilon_{ij} = (1+\nu/E)\sigma_{ij} - \nu/E\sigma_{kk}\delta_{ij} \qquad (4\text{-b})$$

In the equations (4), ν is Poisson's ratio, E is Young's modulus δ_{ij} is Kronecker's delta and summation over repeated indices is assumed. Substituting equation 4-b in equation 2-b:

$$(\epsilon'_{33})_{\phi\psi} = (1+\nu/E)\{\sigma_{11}\cos^2\phi + \sigma_{22}\sin^2\phi + \sigma_{12}\sin 2\phi - \langle\sigma_{33}\rangle_\psi\}\sin^2\psi + (1+\nu/E)$$

$$\langle\sigma_{33}\rangle_\psi - (\nu/E)\sigma_{kk} + (1+\nu/E)\{\langle\sigma_{13}\rangle_\psi\cos\phi + \langle\sigma_{23}\rangle_\psi\sin\phi\}\sin 2\psi \qquad (5)$$

Where carats imply averages over the penetration depth at a particular ψ-angle.

The solution to this equation is given by Dölle[5] where the terms a_1 and a_2 are formed such that:

$$a_1 = \tfrac{1}{2}\{(\epsilon'_{33})_{\phi\psi} + (\epsilon'_{33})_{\phi\psi}\} = (1+\nu/E)\{\sigma_{11}\cos^2\phi + \sigma_{22}\sin^2\phi + \sigma_{12}\sin 2\phi$$

$$-\langle\sigma_{33}\rangle_\psi\}\sin^2\psi - \nu/E\sigma_{kk} + \left(\frac{1+\nu}{E}\right)\langle\sigma_{33}\rangle_\psi \qquad (6\text{-a})$$

$$a_2 = \tfrac{1}{2}\{(\epsilon'_{33})_{\phi\psi} - (\epsilon'_{33})_{\phi\psi}\} = (1+\nu/E)\{\langle\sigma_{13}\rangle_\psi\cos\phi + \langle\sigma_{23}\rangle_\psi\sin\phi\} \cdot$$

$$\sin|2\psi| \; . \qquad (6\text{-b})$$

The stresses $\sigma_{11}, \sigma_{22}, \sigma_{33}, \sigma_{12}$ are then obtained from the slopes and intercepts of a vs. $\sin^2\psi$ for ϕ=0,90,45 respectively. The stresses σ_{13}, σ_{23} are obtained from the slopes of least-squares lines for a_2 vs. $\sin|2\psi|$ for ϕ=0,90.

Equations (6) contain terms (σ_{ij}, i,j=3) which can only exist as gradients in the near surface layers, being, by definition, zero at the surface. Thus, in a strict sense, they violate the condition of homogeneity, required for the use of equations (2). However, assuming that the variation of these stresses are

only along $\underline{S}_3$, and is a single valued function with depth within the penetration distance of X-rays, and that the gradient within the irradiated volume is small, and also assuming that no gradients along $\underline{S}_1$ and $\underline{S}_2$ are present for any element of the stress tensor, it can be shown that the deviation of experimental points from that predicted by equation (2-b) will be small[7,9]. We will call the state described by the above assumptions "quasi-homogeneity" and all the discussion that follows will be based upon these assumptions.

Consider equation (6-b). Since X-rays penetrate to different depths at each ψ-tilt, a different region in the gradient for σ_{13}, σ_{23} will be sampled. This effect when coupled with the fact that $\sin|2\psi|$ is a multi valued function over $\psi=0,60$ (the accessible ψ- range in most experiments), causes non-linearity in a_2 vs. $\sin|2\psi|$. This non-linearity and its effect on the stresses determined from the slope of a_2 vs. $\sin|2\psi|$ lines are now examined.

Assume that the stresses σ_{3j} can be expressed by a power-law in the measurement volume :

$$\sigma_{3j}=a_{3j}\cdot z^{n_{3j}} \qquad (7)$$

where z is the direction coordinate along $\underline{S}_3$, measured into the material and a_{3j} , n_{3j} are constants over the depth of penetration. The average stress value observed by X-rays at any ψ-angle will then be[9]:

$$\langle\sigma_{3j}\rangle_\psi = k_{3j}\tau_\psi^{n_{3j}} \qquad (8)$$

where $\tau_\psi=\sin2\theta\cdot\cos\psi/2\mu$ (9), is the penetration depth of X-rays at any angle for ψ-goniometer geometry.

Substituting (9) into (8) we have:

$$\langle\sigma_{3j}\rangle_\psi=k'(\cos\psi)^{n} \ . \qquad (10)$$

For $\phi=0$, substituting (10) into (6-b) we obtain:

$$(a_2)_\psi = 1+\nu/Ek'_{13}(\cos\psi)^{n_{13}}\cdot\sin|2\psi| \ . \qquad (11)$$

Now let us examine the behaviour of the function $\cos(\psi)^{n_{13}}\sin|2\psi|$. In figure (5-a,b) this behaviour is plotted for $n_{13}=1,2$ respectively. It is seen that:
(i) a_2 vs. $\sin|2\psi|$ is non-linear.
(ii) over a range of $\psi=0,60$ it exhibits splitting. This effect is due to the different regions of the stress gradient sampled at each ψ-tilt. The steeper the gradient, the greater the splitting.
(iii) Three major regions of the a_2 vs. $\sin|2\psi|$ curve may be de-

fined:
a) The low angle region ($\psi < 33.21^{\circ}$ for the cases treated).
b) The apex region ($\psi \in (39.23\text{-}45^{\circ})$).
c) The high angle region($\psi > 50^{\circ}$).

It can be seen from the curves that the slope determined from the low-angle region is smaller than that determined from the high angle region. The slope determined from the apex region is of opposite sign to the slopes determined from the regions a and c.

In order to obtain some magnitudes for these slopes, and the σ_{13} obtained thereof, computer simulation was used. The "d" vs. $\sin^2\psi$ curves were sythesized for a given stress profile, and the results analyzed by least-squares. The following conditions were assumed:

$$\langle\sigma_{13}\rangle_{\psi}=k_{13}\tau_{\psi}^2, \langle\sigma_{33}\rangle_{\psi}=k_{33}\tau_{\psi}^2, (\sigma_{11})_z=(\sigma_{22})_z=-400\text{mPa}$$

The assumed stress profiles are shown in figure 6. The corresponding "d" vs. $\sin^2\psi$ curve is shown in figure 7, with the terms a_1 vs. $\sin^2\psi$, a_2 vs. $\sin|2\psi|$ shown in figures 8-a,8-b respectively. The results of the analysis are summarised in tables I, II.

As was reported earlier[9], the normal stresses σ_{11}, σ_{33} are determined accurately over the high ψ-range. However the stress σ_{13} shown is a totally unrealistic value compared to the actual profile for this region. By comparison, the total range or the lower ψ-range (table I) yield values that are more representative of the average value. However, when the a_2 vs. $\sin|2\psi|$ is divided into the three regions previously defined and analyzed (table II) we see that in comparison to the input profile, the most accurate value is obtained from the low angle region. This is due to the fact that this region best approximates a fit to our starting parameters. In practice however, the angular boundaries of these regions may change depending on the steepness and the shape of the gradient. It is suggested that the complete a_2 vs. $\sin|2\psi|$ plot for $\psi \in (0,60^{\circ})$ for the case at hand be determined before a decision is made over the region of the best linear fit. Alternately, it may be possible to use the shape of the a_2 vs. $\sin|2\psi|$ curve to determine the type of stress gradient in the shear stresses σ_{13}, σ_{23} by determining the best fitting function to the plot using a least squares method[11].

Alignment Errors That Produce ψ-Splitting:

It is well known that positioning of the sample over the center of the diffractometer is critical for the accuracy in the parafocusing method of X-ray residual stress measurement and

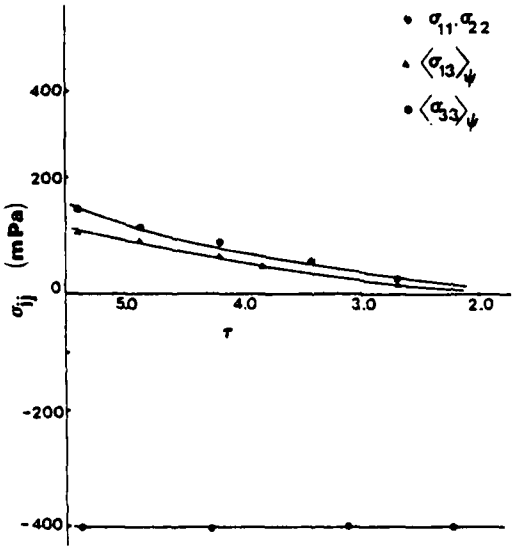

Figure 6: Variation of the (assumed) stresses within the penetration volume in the hypothetical sample.

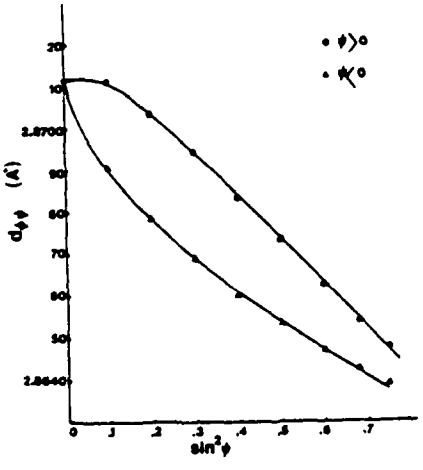

Figure 7: "d" vs. $\sin^2\psi$ profile for a hypothetical steel specimen which has the stress profiles shown in figure 6 in the volume irradiated by X-rays.

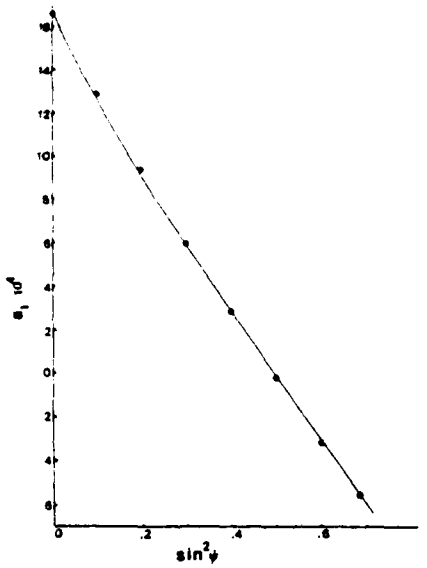

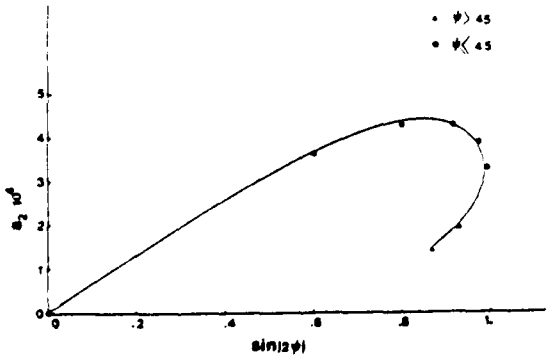

Figure 8: a_1 vs. $\sin^2\psi$ (a) and a_2 vs. $\sin|2\psi|$ (b) profiles calculated from the data shown in figure 7.

Table I: Analysis of the "d" vs. $\sin^2\psi$ curves shown in figure (7) over various ψ-ranges. The (assumed) stress profile is shown in figure (6).

ψ-range	σ_{11}(MPa)	σ_{22}(MPa)	σ_{33}(MPa)	Error in σ_{11}(MPa)	σ_{13}(MPa)	σ_{23}(MPa)
0-60	-442	-442	107	42	50	0
0-33.21	-562	-562	55	162	86	0
39.23-60	-412	-412	81	12	278	0

Table II: Analysis of a_2 vs. $\sin|2\psi|$ curve shown in figure (8-b) over the different ψ-ranges. The assumed stress profile is given in figure (6).

ψ-range	σ_{13}(MPa)	σ_{23}	Corr. Coeff.	Region
0-26-57	96	0	.9952	a
33.21-45.00	-182	0	-.913	b
50.84-60	183	0	.992	c

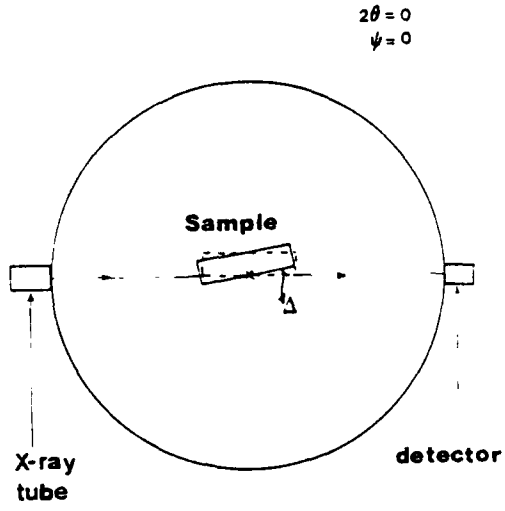

Figure 9: Definition of the "ψ-missetting" for a diffractometer.

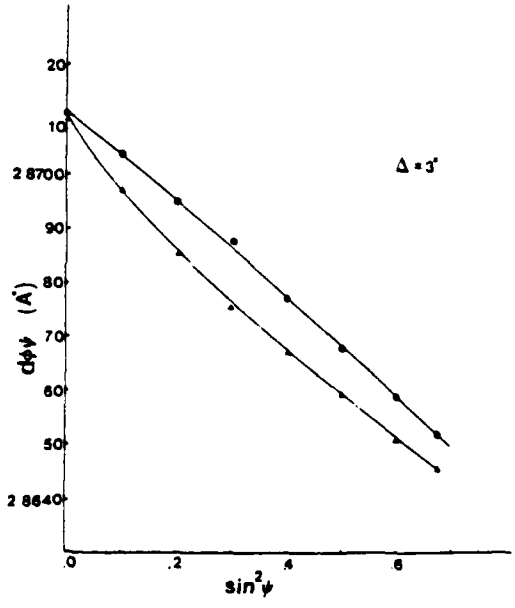

Figure 10: "d" vs. $\sin^2\psi$ for a hypothetical specimen analyzed in a diffractometer with a ψ-missetting of 3 .

that any displacement from the correct position may produce ψ-splitting. Among the various methods used to check this the most widely used is the " stress-free powder " technique in which a (stress-free) powder is dusted on the sample surface and then the sample surface adjusted until no ψ-splitting occurs in the "d" spacings obtained from the powder. It has also been shown that the ψ-splitting shape caused by sample misalignment* is not similar to the shape caused by σ_{13}, σ_{23}. In the following, we will treat an error that can not be detected by the stress-free powder method and gives the same shape for ψ-splitting as equation (2-b):

Assume that the zero position for (ψ-motion), read from the odometer of a diffractometer is different from the geometric definition of zero by Δ degrees, i.e:

$$\psi_{obsv} = \psi_{true} + \Delta \qquad (12)$$

where Δ is defined in figure 9. For a well-aligned diffractometer Δ will be negligible. If, however, the ψ=0 point is not adjusted with the actual (flat) specimen in question Δ up to 1 is possible. With portable residual stress devices coming into use, higher $\Delta$are possible, especially if measurements are being made near fillets, bends etc. Substituting (12) into (5) we obtain: (for σ_{13}, σ_{23}=0)

$$(\epsilon'_{33})_{\phi\psi} = k_\phi(\cos^2\Delta - \sin^2\Delta)\sin^2\psi + k_\phi/2\sin 2\Delta \sin 2\psi + k_\phi \sin^2\Delta + (1+\nu/E)\sigma_{33} - \nu/E\,\sigma_{kk} \qquad (13)$$

$$\text{where } k_\phi = (1+\nu/E)\{\sigma_{11}\cos^2\phi + \sigma_{12}\sin 2\phi + \sigma_{22}\sin^2\phi - \sigma_{33}\}$$

From equation (13) it is seen that an error Δ from the true ψposition will cause splitting proportional to $k_\phi \sin 2\Delta$ for positive and negative ψ. The shape of the split "d" vs. $\sin^2\psi$ curve will be the same shape as predicted by equation (2) with Δ=0 and σ_{13} and/or σ_{23} finite since in both cases the effect is caused by the argument " $\sin 2\psi$".

When all the stress components in equation 13 are zero, as in the case of an annealed powder,

$$(\epsilon'_{33})_{\phi\psi} = d_{\phi\psi} - do/do = 0, \text{ thus, } d_{\phi\psi} = do$$

---

*The equation for the difference in peak shift for a sample displacement ΔX from the center of the diffractometer between an angle ψ and ψ=0 is[18]:

$$\delta(\Delta 2\theta)_{0,\psi} = 360/\ \Delta X \cos\theta\{1/R_{GC} - \sin\theta/R_p^1(\sin\theta+\psi)\}$$

where ΔX is the sample displacement, θ is the Bragg angle, Rgc is the goniometer radius and Rp is given by:

$$R_p^1 = R_{GC}\cdot(\cos(\psi+[90-\theta]))/[\cos[\psi-(90+\theta)]$$

thus, the amount of split between $+\psi$ and $-\psi$ will be: $\Delta\delta(\Delta 2\theta) = \delta(\Delta 2\theta)_{0,\psi} + -\delta(\Delta 2\theta)_{0,\psi}$. The difference is not a function of $\sin 2\psi$.

Table III : Analysis of "d" vs. $\sin^2\psi$ curve shown in figure (10) . (The stress σ_{13} is due to the γ-missetting error in this case.) For this case $\sigma_{11}=\sigma_{12}=-400.$mPa, $\sigma_{33}=k_{33}\sigma x^2$, all other $\sigma_{ij}=0$. The σ_{33} gradient is the same as shown in figure (6).

ψ-range	σ_{11}	σ_{22}	σ_{33}	σ_{13}	σ_{23}	Error in σ_{11}
0-60	-438	-438	107	26	26	38
0-33.21	-556	-556	56	30.5	30.5	156
3923-60	-408	-408	82	56	56	9

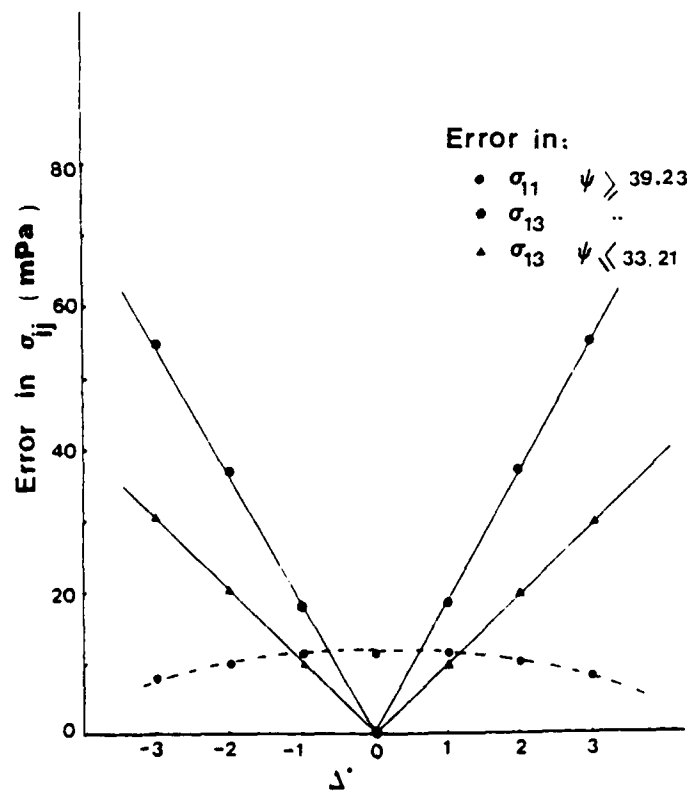

Figure 11: Variation of errors in σ_{11}, σ_{13} with γ-missetting.

for all ϕ, ψ independent of Δ. Thus the stress free powder method of alignment is inadequate to detect the effects due to this error. Verification of the true-zero for movement presents no problem on a diffractometer if a flat sample is used. For curved samples or when a portable unit is used for measurements, a thin sample with known stresses, but no σ_{13}, σ_{27}, that can be placed over the actual measurement surface is needed. An alternative is to rotate ϕ 180°. and repeat the $\mp\psi$ measurements. It can be seen from equations (13) and (5) that while for true ψ-splitting the $d_{\phi\psi}^{+}$, $d_{\phi\psi}$ values will be interchanged, no such change will occur for the missettig case as:

$$k(\phi+180) = k(\phi).$$

Magnitude of Errors Caused By an Error In True Position

Computer simulation was used in this case also. For a given error Δ, the "d" vs. $\sin^2\psi$ plots were synthesized and then analyzed using equations (6-a,b). In figure 10 the "d" vs. $\sin^2\psi$ curve for Δ =3 is shown. The following parameters are used in the data analysis:

$$(\sigma_{11})_z=(\sigma_{22})_z=-400\text{mPa}, \langle\sigma_{33}\rangle_\psi=k_{33}\tau_\psi^2, \text{all other } \sigma_{ij}=0.$$

The σ_{33} gradient is the same as shown in figure 6

The analysis results for figure 10 are shown in table II. It is seen that, as in the first case ($\Delta = 0$, $\sigma_{13} > 0$), the most accurate results for σ_{ij} are obtained from the high ψ-range. The error in σ_{13} (the results in this case are only due to Δ) are highest for this range. This is again due to the interaction of the $\sin|2\psi|$ term with a stress gradient, in this case σ_{33} through k_3 in equation (13). It is also evident that for this case also a_2 vs. $\sin|2\psi|$ will exhibit splitting over $\psi\epsilon(0,60)^\circ$.

In figure 11 the errors in σ_{ij} are plotted as a function of Δ when the high ψ-range is used in the analysis. Also plotted, is the apparent σ_{13} values caused by the presence of Δ versus Δ for both high and low ψ-ranges. It is seen that use of a low ψ-range to evaluate the slope of a_2 vs. $\sin|2\psi|$ line will keep the apparent σ_{13} value below 20 mPa ($\Delta<2^\circ$) which is generally within experimental error.

Conclusions

1) Oscillations in experimentally obtained "d" vs. $\sin^2\psi$ data indicate presence of an inhomogeneous strain state in the surface layers of the sample.

2) The degree of inhomogeneity increases with the magnitude of oscillations and such inhomogeneity causes strain gradients in the surface layers.
3) When large oscillations are present in any one reflection obtained from a given irradiated volume, oscillations can also be present from any other reflection, obtained from the same volume, unless the volume fraction of inhomogeneous regions is small.
4) When strain gradients are only a function of depth in an irradiated volume, a "quasi-homogeneous" strain state may exist if certain other conditions, examined in the text, are fullfilled. In such a case, experimentally determined "d " vs. $\sin^2\psi$ lines deviate slightly from the curves predicted by the equations applicable to homogeneous strain distributions.
5) Even for quasi-homogeneous strain states, application of solutions developed for homogeneous strain states may cause large errors in the stress results if the methods are not appropriately modified for the true strain distribution in the surface layers.
6) Qualitative ideas about the actual strain distribution may be obtained from the deviation of a_1 vs. $\sin^2\psi$ and a_2 vs. $\sin|2\psi|$ plots from linearity. Our examinations here and previously published[9] show that when the quasi-homogeneous gradients in the irradiated volume obey a power law, the stress results obtained from the analysis described by Dolle will be more accurate if;
i) a_1 vs. $\sin^2\psi$ is analyzed over a high ψ-range,
ii) a_2 vs. $\sin|2\psi|$ is analyzed over a low ψ-range.
The linearity of a_2 vs. $\sin|2\psi|$ must be checked for each experiment before the linear range is decided upon.
7) A missetting Δ from the ψ-true-zero position of a diffractometer will cause an apparent ψ-splitting which will have the same shape as a ψ-split caused by the shear stresses σ_{13}, σ_{23}. This error can not be detected by the stress-free powder technique currently in use.
8) The missetting error can be detected by rotating the specimen 180° in ϕ and repeating the measurements for $\mp\psi$. if $(d_{\phi\psi+} = d_{\phi\psi-})_{\phi=\phi+180^\circ}$ then the error is due to misalignment in ψ.

ACKNOWLEDGEMENTS

The financial support for this research was provided by ONR under contract No. N00014-C-0116. The X-ray measurements were made in the diffraction facility of Northwestern University's Materials Research Center, supported in part by the MRL-NSF Program under grant No. DMR-8216972. One of us (I.C. Noyan) thank the Turkish Scientific Research Foundation (TUBITAK) for supplying a NATO grant, enabling him to study in the U.S.A. Also, we thank Mr. Paul Rudnik for help with the x-ray measurements.

REFERENCES

1. B. D. Cullity, Elements of X-ray diffraction, 2nd ed., Addison-Wesley, Reading MA., pp. 447-479 (1978)
2. C. S. Barret, T. B. Massalski, Structure of Metals, 3rd ed., McGraw-Hill, New York, NY, pp. 465-485 (1966)
3. T. Shiraiwa, Y. Sakamoto, X-ray Stress Measurement and Its Application to Steel,Sumito Search, 7:159-169 (1972)
Metall. Trans. A, 11 A: 159 (1980)
4. H. Dölle, J. B. Cohen, Residual Stresses in Ground Steels, Metall. Trans. A, 11 A: 159 (1980)
5. J. W. Ho, I. C. Noyan, J. B. Cohen, V. D. Khanna, Z. Eliezer: Residual Stresses and Sliding Wear, Wear, 84: 183 (1983)
6. H. Dölle, Influence of Multi-Axial Stress States, Stress Gradients and Elastic Anisotropy on the Evaluation of Residual Stresses by X-rays, J. Appl. Cryst. 12: 489 (1979)
7. J. B. Cohen, H. Dölle, M. R. James, Stress Analysis From Powder Diffraction Patterns,National Bureau of Standards Special Publication 567, pp 453-77 (1980)
8. I. C. Noyan, Equilibrium Equations for the Average Stresses measured by X-rays: Met. Trans. A., in print
9. I. C. Noyan, Effect of Gradients in Multi-Axial Stress States on Residual Stress Measurements with X-Rays.Met. Trans. A, 14-A:249(1982)
10. R. H. Marion, J. B. Cohen, Anomalies in Measurement of Residual Stress by X-ray Diffraction,in "Adv. in X-ray Analysis vol. 18" eds. W. 1. Pickles, C. S. Barret, J. B. Newkirk, C. O. Ruud, Plenum, New York, N.Y. (1978) 18: 466 (1975)
11. W. Lode, A. Peiter, Numerik Rontgenographischer Eigenspannungsanalysen Oberflaschennaher Schichten, Harterei Tech. Mitt. 32: 235 (1977)
12. J. F. Nye, Physical Properties of Crystals, Oxford,pp. 3-30.(1976)
13. H. Dölle and J. B. Cohen, Evaluation of (Residual) Stresses in Textured Cubic Materials, Met. Trans. A, 11 A: 831 (1980)
14. S. R. McEwen, J. Faber, A. P. L. Turner, The use of Time-of-flight Neutron Diffraction to the Study of Grain Interaction Stresses,Acta. Met., vol. 31: 657 (1983)
15. K. Hashimoto, H. Margolin, The Role of Elastic Intraction Stresses on the Onset of Slip in Polycrystalline Alpha Brass , Acta. Met. 31: pp. 773-785 (1983)
16. Ibid, , pp. 787-800
17. G. B. Greenough, Residual Stresses in Plastically Deformed Polycryst alline Metal Aggregates, Proc. Roy. Soc., 167-A:556 (1949)
18. M. R. James, Ph. D. Thesis, Northwestern Uni, Evanston, Ill., pp.74 (1977)
19. T. Mura, Micromechanics of Defects in Solids, Martinus Nijhoff, Hague (1982)

Security Classification

DOCUMENT CONTROL DATA - R & D

Security classification of title, body of abstract and indexing annotation must be entered when the overall report is classified)

1. ORIGINATING ACTIVITY (Corporate author)	2a. REPORT SECURITY CLASSIFICATION
J. B. Cohen Northwestern University Evanston, Illinois 60201	Unclassified 2b. GROUP

3. REPORT TITLE

DETERMINING STRESSES IN THE PRESENCE OF NONLINEARITIES IN INTERPLANAR SPACING VS. SIN$^2\psi$

4. DESCRIPTIVE NOTES (*Type of report and inclusive dates*)

Technical Report No. 10

5. AUTHOR(S) (*First name, middle initial, last name*)

I. C. Noyan and J. B. Cohen

6. REPORT DATE	7a. TOTAL NO. OF PAGES	7b. NO. OF REFS
July 29, 1983	23	19

8a. CONTRACT OR GRANT NO	9a. ORIGINATOR'S REPORT NUMBER(S)
N00014-80-C-0116	
b. PROJECT NO Mod. No. P00002	10
c	9b. OTHER REPORT NO(S) (*Any other numbers that may be assigned this report*)
d.	

10. DISTRIBUTION STATEMENT

Distribution of this document is unlimited

11. SUPPLEMENTARY NOTES	12. SPONSORING MILITARY ACTIVITY
	Metallurgy Branch Office of Naval Research

13. ABSTRACT

The sources of non-linearities in interplanar spacing vs $\sin^2\psi$ (used in stress measurements) are clarified.

DD FORM 1 NOV 65 1473 (PAGE 1)

S/N 0101-807-6801

Security Classification

14 KEY WORDS	LINK A		LINK B		LINK C	
	ROLE	WT	ROLE	WT	ROLE	WT
residual stresses, x-ray measurement of residual stresses						

END

DATE
FILMED

9 - 83

DTIC